Available Online: 4 January 2026 DOI: 10.54254/3029-0821/2025.31043

Elucidating early immune signaling pathways underlying chickpea resistance to necrotrophic fungi: a comparative transcriptomic and hormonal analysis

Xingru Meng

The University of Queensland, Brisbane, Australia

mengxingru1999@outlook.com

Abstract. Chickpea is a major protein source in dry and semi-arid regions, but diseases caused by necrotrophic fungi strongly limit yield and the early immune signaling mechanisms remain unclear. This study used one resistant and one susceptible chickpea line inoculated with a dominant Ascochyta isolate and collected leaf samples at 0, 6, 12 and 24 h, combining RNA-seq with quantification of JA, ACC, SA and ABA to compare time-course responses between genotypes. The resistant line showed large-scale transcriptional reprogramming by 12 h with many more up-regulated genes than the susceptible line and strong enrichment in receptor-like kinases, WRKY/ERF transcription factors and cell wall modification pathways. JA and ACC in the resistant line increased rapidly and showed high correlations with key co-expression modules, whereas the susceptible line showed weaker activation and a rise in ABA. The work proposes an early immune signaling framework for chickpea challenged by necrotrophic fungi and identifies a set of candidate hub genes tightly linked to JA/ethylene pathways that can support mechanistic studies and marker-based selection.

Keywords: chickpea, necrotrophic fungi, immune signaling, transcriptomics, phytohormones

1. Introduction

Chickpea is a key grain legume in dry and semi-arid regions and plays an important role in protein supply and sustainable land use, yet diseases caused by necrotrophic fungi, including stem blight, leaf spot and root rot, often lead to severe yield loss and create strong dependence on chemical control while resistant cultivars remain limited [1]. Previous studies have focused on pathogen isolation and virulence characterization and have described population structure and epidemic patterns for several pathogens; classical genetics and QTL mapping have identified some loci linked to resistance, but most work stays at the level of field phenotyping and a few candidate genes and does not resolve host immune events in the first hours after infection [2]. Plant immunity theory suggests that necrotrophic pathogens benefit from host cell death and that the timing of jasmonic acid- and ethylene-centered signaling, reactive oxygen species bursts and cell wall remodeling is critical for resistance, but fine-scale differences in these pathways between resistant and susceptible chickpea genotypes are still unclea [3]. This study therefore uses comparative transcriptomic and hormonal analyses to examine differences in early immune signaling, pathway interactions and key regulatory nodes between

resistant and susceptible chickpea lines and to develop a network framework for early immune signaling during infection by necrotrophic fungi.

2. Literature review

2.1. Disease features of chickpea–necrotroph interactions

Pathological studies on chickpea–necrotroph interactions have revealed that several fungal species dominate in different ecological regions and show distinct specialization patterns, with different Ascochyta and Botrytis isolates producing lesions of contrasting shape, expansion rate and latent period on leaves, stems and pods, which reflects adaptation to tissue types and environmental condition [4]. Inoculation experiments show that spores can complete germination and appressorium formation on the leaf surface within a short time, and that combined action of cuticle disruption and cell wall degrading enzymes accelerates tissue penetration, so that small water-soaked spots rapidly develop into necrotic patches, while rain splash and cultivation operations increase dispersal efficiency [5]. Field monitoring further indicates that fluctuations in temperature and humidity modify the length of the initial infection window and influence divergence in disease progress between genotypes with different resistance levels; some lines with moderate resistance under average conditions become highly susceptible in wet seasons, suggesting that differences in early defense capacity can be amplified by epidemic environments.

2.2. Plant immune signaling pathways and their roles in necrotroph resistance

Studies on plant immune signaling show that PAMP-triggered immunity mediated by pattern recognition receptors and effector-triggered immunity mediated by intracellular receptors form a two-layer structure of defense, in which receptor-like kinases and receptor-like proteins at the plasma membrane activate calcium signaling, reactive oxygen species bursts and MAPK cascades after ligand perception and then drive WRKY, ERF and other transcription factors to remodel defense gene expression patterns [6]. Work on necrotrophic pathogens highlights central roles for jasmonic acid and ethylene signaling in the induction of pathogenesis-related proteins, proteinase inhibitors and cell wall strengthening factors, while salicylic acid often acts antagonistically toward jasmonic acid in many systems and abscisic acid plays a complex role linking osmotic stress responses to certain susceptibility phenotypes [7]. In different crops, necrotrophic pathogens frequently induce local or systemic cell death; hosts must use programmed cell death to form physical barriers yet at the same time restrict excessive death that would supply nutrients to the pathogen, so the temporal and spatial coordination of signaling pathways becomes a key determinant of the split between resistance and susceptibility.

2.3. Applications of integrated transcriptomic and hormonal analyses in crop disease resistance

With the development of high-throughput sequencing and metabolic analysis, many crop–pathogen systems now use transcriptomics to describe genome-wide expression patterns at different disease stages and identify sets of receptors, signaling factors and metabolic enzymes linked to defense through differential expression, clustering and co-expression network analysis, and functional validation has confirmed that some of these genes influence disease outcomes [8]. At the same time, precise quantification of jasmonic acid, salicylic acid, ethylene precursors and abscisic acid allows researchers to match expression modules with hormone dynamics and to analyze differences in hormone combinations and sensitivities between genotypes with different resistance levels [9]; some studies further integrate metabolomics or weighted networks to connect specific

hormone peaks with activation of lignin, flavonoid and alkaloid defense pathways, revealing multi-layer reprogramming from signaling to metabolic effectors.

3. Experimental methods

3.1. Experimental materials and pathogen isolates

One resistant chickpea line R and one susceptible line S selected after multi-year field evaluation under natural disease pressure. Plants grown in a controlled growth chamber to the 6–7 fully expanded leaflet stage under a 16 h light / 8 h dark photoperiod, with day temperature 25 °C, night temperature 20 °C and relative humidity 60%–70%. Pathogen inoculum prepared from a dominant necrotrophic Ascochyta sp. isolate recovered from typical lesions and verified by reinoculation tests. Conidia produced on oatmeal potato agar and suspended at 5×10^5 spores·mL^{-1} with 0.05% Tween-20 to ensure uniform spray coverage. For each genotype, inoculated and water-sprayed control treatments set up with three biological replicates per treatment and at least ten plants per replicate. Immediately after spraying, plants placed in a moist chamber at ≥95% relative humidity for 12 h and then returned to standard chamber conditions, providing sufficient time for spore germination and appressorium formation on the leaf surface. Sampling time points defined as 0, 6, 12 and 24 h post inoculation based on pre-experiments that indicated first visible lesions after this window. At each time point mixed samples of upper fully expanded leaves collected from each treatment–genotype combination. A total of 2 genotypes × 2 treatments × 4 time points × 3 replicates = 48 tissue samples obtained and split for transcriptome sequencing and hormone quantification, forming the basic time-series dataset for later comparisons.

3.2. Sampling design and transcriptome sequencing workflow

Leaves at defined positions cut rapidly at each time point, frozen immediately in liquid nitrogen and stored at –80 °C. Total RNA extracted from all samples within one day. Only RNA with RIN ≥ 7.0 and OD260/280 between 1.9 and 2.1 used for library construction. Each library sequenced on an Illumina platform with 150 bp paired-end reads. Raw read pairs per library not less than 2.8×10^7. Adaptor trimming and low-quality filtering performed with Trimmomatic. Q30 values remained between 93% and 95%. Clean reads aligned to the chickpea reference genome using HISAT2 with overall mapping rates of 89%–92%. Gene-level raw counts generated with featureCounts and used as input for downstream normalization and differential expression analysis in DESeq2. Differentially expressed genes defined by $|\log2 \text{ fold change}| \geq 1$ and Benjamini–Hochberg adjusted FDR < 0.05. For each time point comparisons between inoculated and control samples carried out within R and S separately. Genes with highest variance across all samples (top 5000) used to build weighted gene co-expression networks. Samples clustered according to the “genotype × time × treatment” structure and module eigengenes calculated. Modules with strong correlation to the time gradient retained for later integration with hormone profiles.

3.3. Hormone quantification and signaling pathway validation

Leaf powder (0.20 g) from the same batch of samples used for RNA extraction subjected to hormone extraction. Tissue homogenized in 80% methanol under ice-bath sonication. Extracts centrifuged and purified, then jasmonic acid (JA), the ethylene precursor 1-aminocyclopropane-1-carboxylic acid (ACC), salicylic acid (SA) and abscisic acid (ABA) quantified by UPLC–MS/MS using internal standards [10]. Hormone contents at each time point expressed as fold change relative to the 0 h value. To correct for differences in sequencing

depth between libraries before integration with hormone data, raw gene counts k_{gi} in sample i for gene g normalized by a sample-specific size factor s_i to obtain, as shown in Equation (1).

$$y_{gi}=\frac{k_{gi}}{s_i} \tag{1}$$

And used for module eigengene calculation and correlation analysis. For each co-expression module mmm the eigengene value M_{mt} at time point or sample index t calculated, and Pearson correlation with hormone h content H_{ht} at the same time [11], as shown in Equation (2).

$$r_{mh}=\frac{\sum_{t=1}^{T}\left(M_{mt}-\bar{M}_m\right)\left(H_{ht}-\bar{H}_h\right)}{\sqrt{\sum_{t=1}^{T}\left(M_{mt}-\bar{M}_m\right)^2}\sqrt{\sum_{t=1}^{T}\left(H_{ht}-\bar{H}_h\right)^2}} \tag{2}$$

With $|r_{mh}|\geq 0.7$ and $p < 0.01$ set as thresholds for significant associations. Modules and hub genes showing strong correlation with JA, ACC and other key hormones selected as candidates for early immune signaling components and used as quantitative anchors for the network description in the results section.

4. Results

4.1. Differences in early transcriptional responses and functional enrichment

DESeq2 analysis of the 48 samples used to count up-regulated differentially expressed genes at 6, 12 and 24 h after inoculation in each genotype. Line R showed about 320 up-regulated genes at 6 h, 1483 at 12 h and 1356 at 24 h. Line S showed only 112, 624 and 587 up-regulated genes at the same time points. A line plot of these values (Figure 1) revealed a steep peak for R at 12 h, whereas the curve for S remained relatively flat. Within the 1483 up-regulated genes in R at 12 h, functional annotation identified 214 receptor-like kinase genes, 76 WRKY or ERF transcription factor genes and 189 genes involved in cell wall polysaccharide synthesis and modification, together accounting for 32.0% of all up-regulated genes at this time point. In S, genes in the same functional categories totaled fewer than 130 and accounted for only 20.8% of its up-regulated genes. Variance-stabilizing transformation of expression values followed by principal component analysis produced a first principal component (PC1) explaining 41.2% of total variance, mainly separating inoculated and control samples, and a second principal component (PC2) explaining 18.7% of variance, reflecting genotype differences. Inoculated R samples at 12 h showed the strongest displacement along both PC1 and PC2, indicating concentrated and pronounced rearrangement of genome-wide expression patterns at this time in the resistant genotype.

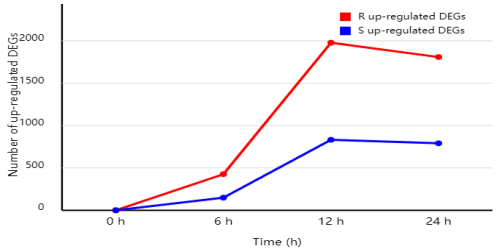

Figure 1. Changes in the number of up-regulated differentially expressed genes in resistant (R) and susceptible (S) chickpea lines at different time points after inoculation

4.2. Hormone dynamics and construction of an immune signaling network

UPLC–MS/MS quantification of JA, ACC, SA and ABA carried out on the same set of samples used for transcriptomics. Hormone contents at each time point converted to fold changes relative to 0 h, and mean ± standard error calculated for each genotype with n = 3. Values summarized in Table 1. In line R, JA reached 2.46 ± 0.18-fold at 12 h and ACC reached 1.85 ± 0.14-fold, both showing stepwise increases between 6 and 12 h. In line S, JA reached only 1.23 ± 0.11-fold and ACC only 1.09 ± 0.08-fold at 12 h. SA in R increased from 12 h onward to 1.41 ± 0.11-fold at 24 h, whereas ABA remained slightly below baseline, between 0.87 ± 0.07 and 0.90 ± 0.08. In S, ABA increased to 1.21 ± 0.10-fold at 12 h and 1.18 ± 0.09-fold at 24 h. Correlation analysis between these time-series hormone profiles and the module eigengenes from Section 3.3 indicated that in R, JA showed a correlation coefficient $r = 0.82$ ($p < 0.001$) with a module enriched in WRKY and ERF transcription factors and cell wall modification genes, and ACC showed $r = 0.79$ with the same module. In S, the corresponding correlation coefficients were 0.41 and 0.38 and did not pass the significance threshold. A third module where POD and LAC genes have a strong presence showed correlation coefficients of 0.76 with SA in the resistant genotype (R) and 0.52 in the susceptible genotype (S). Along with these, results obtained in Table 1 show that with respect to SA fold change, the temporal response of this particular module corresponds more to the dynamic change in SA in R. Simultaneously with this increase in ABA in S, a small module primarily specifying genes involved in stress responses showed a correlation of $r = 0.69$ with ABA.

Table 1. Relative contents (fold change, mean ± standard error, n = 3) of key hormones in resistant (R) and susceptible (S) chickpea lines at different time points after inoculation

Hormone	Line	0 h	6 h	12 h	24 h
JA	R	1.00 ± 0.00	1.78 ± 0.15	2.46 ± 0.18	2.10 ± 0.17
JA	S	1.00 ± 0.00	1.12 ± 0.10	1.23 ± 0.11	1.18 ± 0.09
ACC	R	1.00 ± 0.00	1.42 ± 0.12	1.85 ± 0.14	1.67 ± 0.13
ACC	S	1.00 ± 0.00	1.05 ± 0.08	1.09 ± 0.08	1.07 ± 0.07
SA	R	1.00 ± 0.00	1.08 ± 0.09	1.32 ± 0.10	1.41 ± 0.11
SA	S	1.00 ± 0.00	1.03 ± 0.07	1.05 ± 0.09	1.06 ± 0.08
ABA	R	1.00 ± 0.00	0.95 ± 0.07	0.87 ± 0.07	0.90 ± 0.08
ABA	S	1.00 ± 0.00	1.11 ± 0.09	1.21 ± 0.10	1.18 ± 0.09

5. Discussion

This study compared early responses of resistant and susceptible chickpea lines under unified inoculation conditions. The results showed that the resistant line displayed stronger transcriptional reprogramming between 6 and 12 h, with up-regulated genes concentrated in receptor-like kinase, WRKY/ERF and cell wall modification pathways. Fold changes of JA and ACC showed higher correlations with defense co-expression modules than in the susceptible line, while SA increased slightly and ABA was suppressed, forming a necrotroph-defense pattern dominated by JA/ethylene. The susceptible line showed lower JA/ACC peaks together with rising ABA, which resembled a general stress response rather than a targeted defense. These findings indicate that resistance depends on temporal coordination across multiple modules rather than simple high expression of a few defense genes.

6. Conclusion

This study focused on the early stage of chickpea infection by a necrotrophic fungus and built an integrated "resistant/susceptible genotypes × multiple time points × transcriptome–hormone" analysis framework to compare pathway reorganization under the same pathogen pressure. The resistant line showed synchronous up-regulation of receptor-like kinases, WRKY/ERF transcription factors and cell wall modification genes around 12 h that tightly matched JA and ACC peaks, whereas the susceptible line showed weaker activation of defense genes and stronger engagement of an ABA-linked stress module. The results support an early immune model centered on JA/ethylene, with moderate SA and limited ABA, and provide a set of hub genes that are specifically reinforced in the resistant background. These genes represent priority targets for further studies on resistance mechanisms and for the development of molecular markers.

References

[1] Jha, U. C., et al. (2022). Breeding and genomics interventions for developing Ascochyta blight resistant grain legumes. *International Journal of Molecular Sciences, 23*(4), 2217.

[2] Deokar, A. A., Sagi, M., & Tar'an, B. (2024). Genetic analysis of partially resistant and susceptible chickpea cultivars in response to Ascochyta rabiei infection. *International Journal of Molecular Sciences, 25*(2), 1360.

[3] Raman, R., et al. (2024). Metabolite profiling of chickpea (Cicer arietinum) in response to necrotrophic fungus Ascochyta rabiei. *Frontiers in Plant Science, 15*, 1427688.

[4] Dariva, F. D., et al. (2024). Identification of novel candidate genes for Ascochyta blight resistance in chickpea. *Scientific Reports, 14*(1), 31415.

[5] Farahani, S., et al. (2022). Genome-wide association mapping for isolate-specific resistance to Ascochyta rabiei in chickpea (Cicer arietinum L.). *Physiological and Molecular Plant Pathology, 121*, 101883.

[6] Şahin, E. S., et al. (2023). Genome wide association study of genes controlling resistance to Didymella rabiei Pathotype IV through genotyping by sequencing in chickpeas (Cicer arietinum). *Genomics, 115*(5), 110699.

[7] Carmona, A., et al. (2023). Genomic data of two chickpea populations sharing a potential Ascochyta blight resistance region. *Data in Brief, 50*, 109624.

[8] Yadav, P., et al. (2023). Comprehensive transcriptome analyses of Fusarium-infected root xylem tissues to decipher genes involved in chickpea wilt resistance. *3 Biotech, 13*(12), 390.

[9] Soltabayeva, A., et al. (2022). Receptor-like kinases (LRR-RLKs) in response of plants to biotic and abiotic stresses. *Plants, 11*(19), 2660.

[10] Rehman, M., et al. (2023). The multifaceted role of jasmonic acid in plant stress mitigation: an overview. *Plants, 12*(23), 3982.

[11] Macioszek, V. K., et al. (2023). Jasmonic acid as a mediator in plant response to necrotrophic fungi. *Cells, 12*(7), 1027.